

## Quantum Monte Carlo method for models of molecular nanodevices

Liliana Arrachea<sup>1,2</sup> and Marcelo J. Rozenberg<sup>2,3</sup>

<sup>1</sup>*Instituto de Biocomputacion y Fisica de Sistemas Complejos, Universidad de Zaragoza, Corona de Aragon 42 (50009) Zaragoza, Spain*

<sup>2</sup>*Laboratoire de Physique des Solides, CNRS-UMR8502, Universite de Paris-Sud, Orsay 91405, France*

<sup>3</sup>*Departamento de Física, FCEN, Universidad de Buenos Aires, Ciudad Universitaria Pab. 1, 1428 Buenos Aires, Argentina*

(Received 16 March 2004; revised manuscript received 8 April 2005; published 5 July 2005)

We introduce a quantum Monte Carlo technique to calculate exactly at finite temperatures the Green function of a fermionic quantum impurity coupled to a bosonic field. While the algorithm is general, we focus on the single impurity Anderson model coupled to a Holstein phonon as a schematic model for a molecular transistor. We compute the density of states at the impurity in a large range of parameters, to demonstrate the accuracy and efficiency of the method. We also obtain the conductance of the impurity model and analyze different regimes. The results show that even in the case when the effective attractive phonon interaction is larger than the Coulomb repulsion, a Kondo-like conductance behavior might be observed.

DOI: [10.1103/PhysRevB.72.041301](https://doi.org/10.1103/PhysRevB.72.041301)

PACS number(s): 73.63.-b, 02.70.Ss, 71.10.-w

The physics of quantum impurities is attracting a great deal of attention. For decades, their study has been a classic subject in the area of strongly correlated electron systems.<sup>1</sup> However, with the dramatic recent advances in nanoscale physics their interest has become paramount to a much broader audience. Among the most interesting recent achievements in nanometer-scale devices we find the ability to attach individual molecules to metallic electrodes.<sup>2</sup> In these systems, the coupling between the discrete internal degrees of freedom of the molecule and the macroscopic leads gives rise to transport channels enabled by resonances originated in many-body interactions. An important example is the observation of the physics of the Kondo effect,<sup>3</sup> which were previously seen in quantum dots.<sup>4</sup> In general, one expects that the transport through molecular devices will be affected by the coupling between their internal vibration modes and the electrons.<sup>2</sup> In addition, one should also consider the possible electron correlation effects due to Coulomb repulsion within the molecule.<sup>3</sup>

The solution of quantum impurity models has remained a difficult task,<sup>1</sup> and exact solutions are only possible in very specific instances with the use of techniques such as the Bethe ansatz. For general models, however, theoreticians have to rely heavily on numerical methods. Among those we count the celebrated Wilson's numerical renormalization group (NRG) and its various generalizations.<sup>1</sup> This method is extremely accurate for the determination of the low energy physics of the model, but has limitations for the investigation of intermediate temperatures and impurity models with many orbitals. On the other hand, there is a very efficient quantum Monte Carlo (QMC) method introduced by Hirsch and Fye<sup>5</sup> that does not present those limitations and neither the so-called "negative sign" problem.

Among the models of quantum impurities, a most important one is the single impurity Anderson model (SIAM) Hamiltonian,<sup>6</sup> that has been crucial for a large number of physical problems. Essentially it consists of an atomic orbital (the impurity) with an on-site repulsive Coulomb interaction that is hybridized with a band of conduction electrons.

The goal of the present paper is twofold: we shall first present an algorithm that generalizes that of Hirsch and Fye

to the quantum impurity problem of a SIAM coupled to a general bosonic field. In order to test our method we shall consider the particular case of the SIAM coupled to a Holstein phonon that has been recently studied with NRG at  $T=0$ . We shall present the detailed behavior of the density of states (DOS) of the impurity for various phonon strengths, local Coulomb interactions, and temperatures. The second goal of our paper will be to discuss results for the conductance of this quantum impurity as a function of the gate voltage, that can be understood under the light of our DOS calculations. We shall show the two generic conductance behaviors that occur depending on the values of the parameters. Our results should be useful for the interpretation of experiments of transport through molecular transistors.

The SIAM coupled to a general bosonic mode is described by the action

$$\begin{aligned} \mathcal{S} = & \sum_{\sigma} \int d\tau d\tau' \bar{c}_{\sigma}(\tau) G_0^{-1}(\tau - \tau') c_{\sigma}(\tau') + \int d\tau d\tau' \phi(\tau) D_0^{-1} \\ & \times (\tau - \tau') \phi(\tau') + \int d\tau U n_{\uparrow}(\tau) n_{\downarrow}(\tau) + \lambda \sum_{\sigma} \int d\tau \phi(\tau) \\ & \times \left( \bar{c}_{\sigma}(\tau) c_{\sigma}(\tau) - \frac{1}{2} \right), \end{aligned} \quad (1)$$

where  $\bar{c}_{\sigma}, c_{\sigma}$  are Grassmann variables for the creation and destruction of an electron with spin  $\sigma$  at the impurity and  $\phi$  is the bosonic field. The coupling  $\lambda$  is the strength of the interaction between the electrons at the impurity and the bosonic degree of freedom, and  $U$  is the Coulomb cost for the double occupation of the impurity site. The noninteracting propagators are  $D_0(\omega_m)$  for the bosons and  $G_0(\omega_n) = [i\omega_n - V_g + \Delta(\omega_n)]^{-1}$  for the impurity electrons, being  $\omega_m$  and  $\omega_n$  bosonic and fermionic Matsubara frequencies respectively. The hybridization function  $\Delta(\omega_n)$  describes the coupling to the (given) conduction band and  $V_g$  denotes the gate voltage.

We shall now describe the QMC algorithm. As usual one performs a Trotter breakup of imaginary time into  $M$  time

slices  $\tau_l$  of length  $\Delta\tau=\beta/M$  to discretize the action (1) and introduce a discrete Hubbard-Stratonovich transformation with auxiliary Ising-like fields  $s_l, l=0, \dots, M-1$ .

This renders the action quadratic in the fermionic variables that can be integrated out. The resulting partition function is

$$Z = \text{Tr}_{\{s_l\}} \int \mathcal{D}\phi \text{Det}[G_{\uparrow}^{-1}(\tau_l, \tau_{l'})] \text{Det}[G_{\downarrow}^{-1}(\tau_l, \tau_{l'})] \exp \left\{ \frac{1}{\beta} \sum_m \bar{\phi}_m^* D_0^{-1}(i\omega_m) \bar{\phi}_m + \lambda \bar{\phi}_0 \right\}, \quad (2)$$

where  $\bar{\phi}_m$  are the Fourier transform components of the bosonic field that obey  $\bar{\phi}_m = \bar{\phi}_{-m}^*$ . The  $s_l$  and  $\phi_m$  dependent electron Green functions are<sup>7</sup>

$$G_{\sigma}^{-1}(\tau_l, \tau_{l'}) = G_0^{-1}(\tau_l - \tau_{l'}) + \delta_{l,l'} [\sigma \lambda_U s_l + \Delta\tau \lambda \phi(\tau_l)], \quad (3)$$

with  $\cosh \lambda_U = \exp(\Delta\tau U/2)$ . A crucial aspect of our algorithm is the choice of a simultaneous representation in terms of the Ising-like and *continuous* bosonic fields. Other algorithms chose to integrate out the bosonic variables to obtain a time-dependent electron density-density interaction that is then decoupled via a *single* continuous Hubbard-Stratonovich field. That procedure gives up the very nice properties of the discrete Ising-like fields and should be expected to have serious autocorrelation problems. In the present case, each degree of freedom is simulated in the most effective way. This is evident for the Ising fields, but should also be clear for the bosonic fields as our frequency modes representation is reminiscent of the Fourier acceleration method. In fact, while the update of the Ising fields is known to lead to very short autocorrelation times, the same is not true for the bosonic fields. The physical reason is that the most relevant bosonic configurations are those in which  $\phi(\tau)$  have a slow variation with  $\tau$ . To generate those configurations one needs to propose moves that coherently and unbiased involve all the  $M$  variables  $\phi(\tau_l)$ . Our algorithm provides a systematic way to do this by updating the frequency components  $\bar{\phi}_m$  of the bosonic fields. It is important to mention that the autocorrelation times of  $\bar{\phi}_m$  remain pretty long (typically about a hundred sweeps) but, unlike what would be updating in a time domain, practically tractable.

The integrand of (2) thus defines the Boltzmann weight  $\mathcal{W}[s_l; \bar{\phi}_m]$  for the stochastic evaluation of the trace on the Ising and bosonic fields. We use a heat-bath algorithm according to which new configurations  $\{s_l; \bar{\phi}_m\}$  are generated and accepted with a probability  $P(\mathcal{W} \rightarrow \mathcal{W}') = \mathcal{W}' / (\mathcal{W}' + \mathcal{W})$ . The ensuing Markov chain is: (i) Each Ising variable is visited and a flip  $s_l \rightarrow -s_l$  is proposed. The acceptance of the move is evaluated as in the usual Hirsch and Fye algorithm<sup>5</sup> and the new Green function can be computed in  $O(M^2)$  operations. (ii) Every independent complex variable  $\bar{\phi}_m = (\bar{\phi}_m^R, \bar{\phi}_m^I)$  is visited and a move  $\bar{\phi}_m^{R,I} \rightarrow \bar{\phi}_m^{R,I} + \delta_m^{R,I}$  is proposed, with  $\delta_m^{R,I} \in [-\Lambda, \Lambda]$  a uniformly distributed random number. After Fourier transforming back  $\bar{\phi}$ , the update re-

quires a full matrix inversion (3), that is  $O(M^3)$  operations.<sup>10</sup> One can verify that, similarly as the original Hirsch and Fye algorithm, this procedure fulfills detailed balance:  $\mathcal{W}P(\mathcal{W} \rightarrow \mathcal{W}') = \mathcal{W}'P(\mathcal{W}' \rightarrow \mathcal{W})$ .

Holstein phonons are bosonic fields defined by its noninteracting correlation function  $D_0(i\omega_m) = -2\Omega_0 / (\omega_m^2 + \Omega_0^2)$ , where  $\Omega_0$  is the phonon frequency. For the electron conduction band that is hybridized with the impurity we shall take a semicircular density of states, thus  $\Delta(\omega)/2 = t_c^2 \rho_0(\omega) = 4t_c^2 \sqrt{W^2 - \omega^2} / W^2$  with  $\rho_0(\omega)$  the conduction electron DOS,  $W$  its half-bandwidth and  $t_c$  is the hybridization coupling. The choice of a semicircular DOS is made because it would also be appropriate for our investigation of conductance through the impurity. In fact, the same  $\Delta(\omega)$  also results from attaching two leads to the impurity in the form of two semi-infinite chains of atoms with intersite hopping amplitude  $W/2$ . This setup is usually used for modeling nanodevices, such as a molecule connected to two metallic leads.

The DOS at the impurity  $\rho(\omega) = -2 \text{Im}[G_{\sigma}(\omega)]$  is obtained by a maximum entropy method for the analytic continuation of the QMC-calculated Green function to the real frequency axis. We typically use up to 64 time slices and 200 000 complete sweeps of the statistical fields. We consider first the simpler case of  $U=0$  and show in Fig. 1 systematic results for fixed  $\lambda$  and increasing phonon frequency  $\Omega_0$ . For the analysis of the results it is useful to recall that within the static approximation [i.e., taking  $D_0(i\omega_m) \approx D_0(i\omega_0) \delta_{0,m}$ ], which becomes more accurate in the small  $\Omega_0$  limit, the integration of the bosons leads to an effective interaction between the electrons  $-U_{eff} = -2\lambda^2 / \Omega_0$ . Since it is attractive, and our model is particle-hole symmetric, it will favor an empty or doubly occupied impurity state. Adding or removing an electron from the impurity has an energy cost of  $\sim U_{eff}/2$ , which is, in fact, the position of the two features in the DOS of the top panel of Fig. 1 for the smaller  $\Omega_0 = 0.333$ . As  $\Omega_0$  is increased and  $U_{eff}$  decreases, the DOS at low frequency has a dramatic enhancement with a strong quasiparticle peak emerging at  $\omega=0$ . This resonance corresponds to slow charge fluctuations at the impurity and is the charge counterpart of the Kondo effect. At higher frequencies a richer peak structure also evolves, where the two side peaks of the Kondo-like resonance correspond to the (dynamically renormalized)  $U_{eff}/2$  features, while the two additional peaks at higher frequency  $\omega \approx \pm (U_{eff}/2 + \Omega_0)$  correspond to adding (or removing) a particle plus a phonon. When  $\Omega_0$  is further increased (diminishing  $U_{eff}$ ), charge fluc-

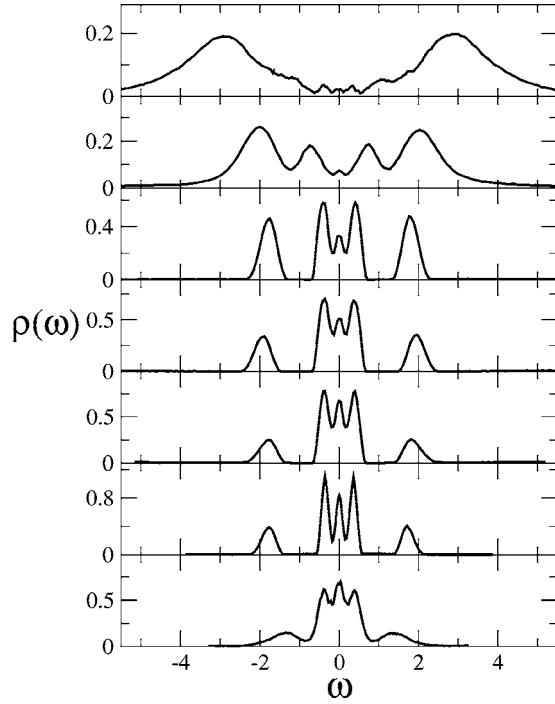


FIG. 1. DOS for  $U=0$ ,  $W=8$ ,  $t_c=1.0$ , and  $T=0.0357$ . Other parameters are:  $\lambda=1$ ,  $\Omega_0=0.333, 0.5, 0.75, 1.0, 1.5, 2.0$ , and  $\lambda=0.5$ ,  $\Omega_0=2$  (upper to lower panel).

tuations are no longer prevented and the DOS moves towards that of a simple resonant level model with just a remnant substructure at frequencies  $\omega \sim \Omega_0$ . This basic systematic behavior is consistent with the  $T=0$  numerical studies using NRG.<sup>8</sup>

We now turn to the evolution of the DOS as a function of  $T$  shown in Fig. 2. At high temperatures (upper panel) strong charge fluctuations dominate and the DOS is that of a reso-

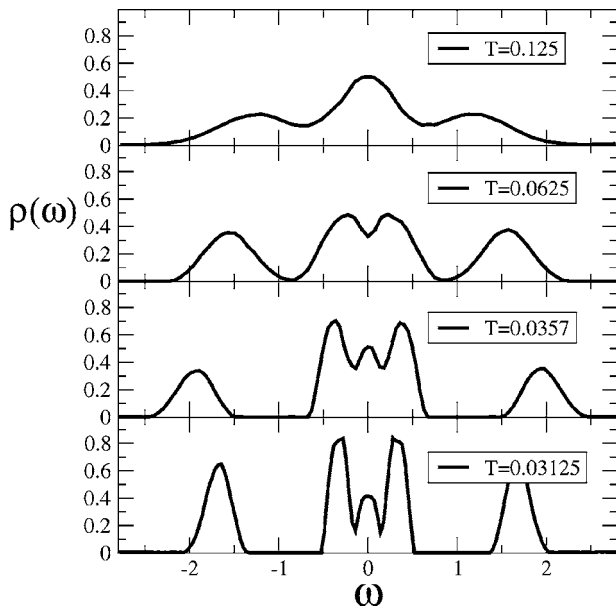


FIG. 2. Behavior of the DOS with  $T$  for  $\lambda=1$  and  $\Omega_0=1$ . Other parameters are as in Fig. 1.

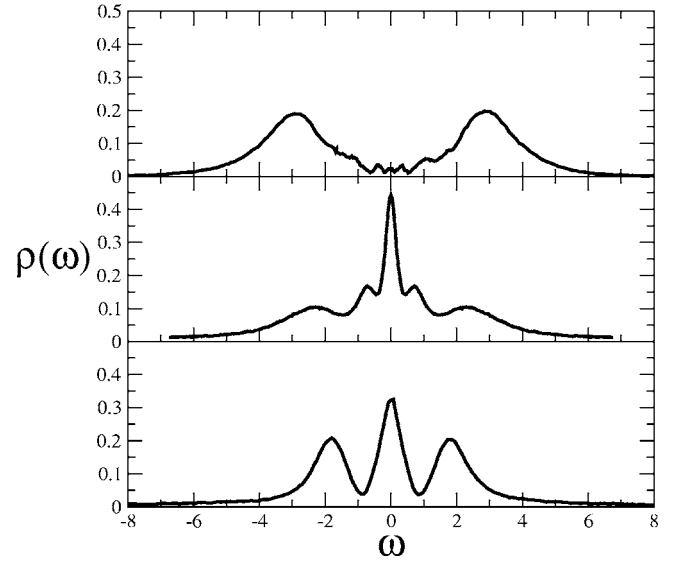


FIG. 3. Top: DOS without Coulomb repulsion ( $U=0$ ,  $\lambda=1$ ). Bottom: DOS without phonons ( $U=4$ ,  $\lambda=0$ ). Middle: DOS with Coulomb repulsion and phonons ( $U=4$ ,  $\lambda=1$ ). The phonon frequency is  $\Omega_0=0.333$ ,  $T=0.0357$  (top), and  $T=0.0625$  (middle and bottom).

nant model with a strong and broad feature at  $\omega=0$ . In addition, two side peaks are present at  $\omega \sim \pm\Omega_0$  due to excitations to states with an additional phonon. Lowering  $T$  we observe that the central feature splits up into two peaks. This splitting occurs due to the thermal selection of the more favorable empty and doubly occupied states as thermal charge fluctuations decrease. Finally (two lower panels), below  $T_\lambda \sim 0.0625$  (analogous to the Kondo temperature), a strong resonance reemerges at  $\omega=0$  due to the Kondo-like mechanism in the charge sector. From the Kondo model analogy,  $T_\lambda \propto \exp(-U_{eff})$  therefore is rapidly suppressed with increasing  $\lambda$  or decreasing  $\Omega_0$ .

We now switch on the interaction  $U$  and observe the interplay between the usual Kondo effect and the vibrational modes (Fig. 3). Without phonons, i.e.,  $\lambda=0$  (bottom) the DOS consists of a central Kondo resonance and side features at  $\pm U/2$ . The familiar Kondo peak is due to slow fluctuations between the spin-up and spin-down states within the charge sector of single occupation. Upon coupling to the vibrational modes, the effective electronic interaction of the impurity becomes dynamical and strongly renormalized (screened). Within the static approximation, its value becomes  $U_{dyn}=U-U_{eff}=U-2\lambda^2/\Omega_0$ . The effective phonon interaction can even render the interaction attractive as in the case of superconductivity. The effect on the impurity DOS is quite notable (middle), renormalizing the side peaks to  $\omega \sim \pm U_{dyn}/2$  and adding higher frequency peaks due to additional phonon excitation. A central Kondo-like resonance remains, however, it is now due to a rather complicated many body state involving both slow spin and charge fluctuations.

We may now turn to the discussion of the consequences of the above-mentioned effects on the conducting properties of this quantum impurity model that should be relevant for nanoscopic devices such as a molecule attached to leads with both electronic and vibrational degrees of freedom.

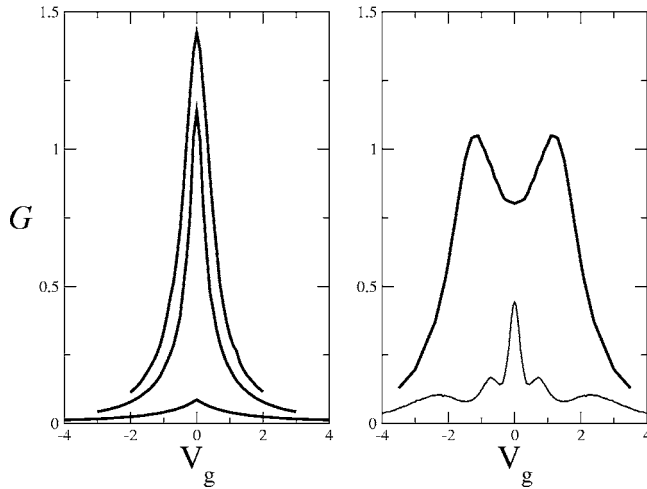


FIG. 4. Conductance (a.u.) at  $T=0.0625$  and  $\lambda=1$  as a function of the gate potential  $V_g$ . Left:  $U=0$  and  $\Omega_0=0.333, 1, 2$  (bottom to top). Right:  $U=4$  and  $\Omega_0=0.333$ . For comparison, in the thin line we show  $\rho(\omega)$  for  $V_g=0$ .

One of the usual experimental setups to study transport phenomena in nanostructures,<sup>2-4</sup> consists in applying a bias potential between the left and the right sides of the impurity (molecule), and then measuring the current through it. In addition, a gate voltage  $V_g$  might be applied at the impurity site and the conductance is obtained as a function of  $V_g$ .

In the limit of very small bias between the left and right leads the conductance can be calculated from<sup>9</sup>

$$G = \frac{e}{2\hbar} \sum_{\sigma} \int \frac{d\omega}{2\pi} t_c^2 \rho_0(\omega) \frac{\partial f(\omega)}{\partial \omega} \rho(\omega), \quad (4)$$

where  $f(\omega)=1/(1+e^{\beta\omega})$ . Results at low  $T$  are shown in Fig. 4. In this parameter regime, the behavior of  $G$  is essentially given by the value of  $\rho(0)$ . For  $U=0$  (left) a maximum in the conductance is observed at  $V_g=0$ , and its value is strongly enhanced as  $U_{eff}$  is decreased. The maximal value of the conductance is controlled by the spectral strength of the

Kondo-like resonance that is rapidly suppressed by  $U_{eff}$ . While the  $V_g=0$  case is understood in terms of the analogy to the usual Kondo case, we find that upon application of a gate potential there is a very different behavior with respect to the case of conductance through a magnetic impurity. In the latter case, at low  $T$ , the conductance display peaks at  $\pm U/2$  and remains sizable in between.<sup>4</sup> This is because the Kondo peak survives the departure from the particle-hole symmetric situation, since  $V_g$  does not break the spin doublet at the impurity and the slow spin fluctuation mechanism remains operational. In stark contrast, the present case shows a rather narrow peak of the conductance centered at  $V_g=0$  and this is due to the fact that a finite  $V_g$  immediately destroys the empty-doubly occupied doublet at the impurity, and the validity of the Kondo-like analogy. At low temperatures, the probability of the participation of those states differs by a factor  $\sim \exp(-V_g/T)$ . Switching on  $U$  (right), we find a new surprise, namely that even for  $U_{dyn}<0$  (i.e., the phonon-mediated interaction dominates) the conductance remains high in a neighborhood of  $V_g=0$  and develops a two-peak structure at  $V_g \approx \pm U_{dyn}/2$ . This behavior is consistent with a Kondo-like character that remains present even away from particle-hole symmetry. The systematic investigation of the conductance in the whole parameter regime is left for future investigations.

In conclusion, we have presented a QMC algorithm for the numerical solution of a general class of quantum impurities models with fermionic and bosonic degrees of freedom. We considered the specific case of a SIAM with a Holstein phonon that served both to benchmark the quality of our method and to demonstrate different effects in the impurity conductance. This model and further generalizations might be of great help for the investigation of conduction properties through molecular nanodevices.

We thank P. Fulde for his hospitality at the MIPKs-Dresden as well as D. Grempel, P. Cornaglia, and Y. Kakehashi for useful conversations. We acknowledge support from CONICET and PICT 03-11609 of Argentina and L.A. from MCyT Spain under RyC program.

<sup>1</sup>A. C. Hewson, *The Kondo Problem to Heavy Fermions*, Cambridge Studies in Magnetism Vol. 2 (Cambridge University Press, Cambridge, 1993).

<sup>2</sup>H. Park *et al.*, Nature (London) **407**, 57 (2000).

<sup>3</sup>J. Park *et al.*, Nature (London) **417**, 722 (2002); W. Liang *et al.*, Nature (London) **417**, 725 (2002); L. H. Yu *et al.*, Phys. Rev. Lett. **93**, 266802 (2004).

<sup>4</sup>D. Goldhaber-Gordon *et al.*, Nature (London) **391**, 156 (1998).

<sup>5</sup>J. E. Hirsch and R. M. Fye, Phys. Rev. Lett. **56**, 2521 (1986).

<sup>6</sup>P. W. Anderson, Phys. Rev. **124**, 41 (1961).

<sup>7</sup>In the actual implementation we use a similar Dyson formula expression as in.<sup>5</sup> This simpler expression is used here the sake of clarity.

<sup>8</sup>A. C. Hewson and D. Meyer, J. Phys.: Condens. Matter **14**, 427 (2002); D. Meyer, A. C. Hewson, and R. Bulla, Phys. Rev. Lett. **89**, 196401 (2002); P. S. Cornaglia, H. Ness, and D. R. Grempel, *ibid.* **93**, 147201 (2004).

<sup>9</sup>Y. Meir and N. S. Wingreen, Phys. Rev. Lett. **68**, 2512 (1992).

<sup>10</sup>While this may seem a drawback, in practice it turns out that not visiting the high- $m$  bosonic fields usually does not degrade the quality of the numerical results.